

- Program Selection*, J. Kien, C. R. McCrohan, W. Winlow, Eds. (Pergamon, Oxford, 1992), pp. 105–122; J. Kein and J. S. Altman, *ibid.*, pp. 147–169; W. B. Kristan, G. Wittenberg, M. P. Nusbaum, W. Stern-Tomlinson, *Experientia* 44, 383 (1988); S. R. Soffe, in *Neurobiology of Motor Program Selection*, J. Kien, C. R. McCrohan, W. Winlow, Eds. (Pergamon, Oxford, 1992), pp. 73–87; W. J. Heitler, *J. Exp. Biol.* 114, 521 (1985); F. Baldissera, H. Hultborn, M. Illert, *Handbook of Physiology: The Nervous System* (William and Wilkins, Baltimore, MD, 1981); S. R. Lockery and W. B. Kristan Jr., *J. Neurosci.* 10, 1811 (1990).
6. Preliminary observations [C. X. Falk, H. P. Hopp, J.-y. Wu, L. B. Cohen, *Soc. Neurosci. Abstr.* 15, 1264 (1989)] suggest that sensory feedback resulting from the gill movement in the withdrawal reflex is undetectable in voltage-sensitive dye recordings from the *Aplysia* abdominal ganglion.
 7. Voltage-sensitive dyes and 124 elements of a 12 by 12 array of silicon photodiodes were used to simultaneously monitor up to 30% of the neurons in the ganglion. The isolated siphon preparation [I. Kupfermann, H. Pinsker, V. Castellucci, E. R. Kandel, *Science* 174, 1252 (1971)] dissected from adult animals (5 to 10 g) was used. The abdominal ganglion was stained with the voltage-sensitive, pyrazolone-oxonol dye NK3041 [A. Grinvald, R. Hildesheim, R. Gupta, L. B. Cohen, *Biol. Bull.* 159, 484 (1980)] obtained from Nippon Kankoh Shikiso Kenkyusho, Okayama, Japan. This dye was first suggested and synthesized by R. Hildesheim and A. Grinvald as RH155. To obtain the identification numbers given on the left of Figs. 2 and 3, we used the detector number that had the largest signal from that neuron. If a detector was used for recording the activity of more than one neuron, we added 1000 to the identification number for each reuse. We monitored the gill movements by plotting the area of the gill as a function of time using a video image integrator. Additional details of the experimental procedures have been described (4) [C.-X. Falk, J.-y. Wu, L. B. Cohen, A. Tang, *J. Neurosci.* 13, 4072 (1993); L. B. Cohen and S. Leshner, *Soc. Gen. Physiol. Ser.* 40, 71 (1986)].
 8. R. E. Coggeshall, *J. Neurophysiol.* 30, 1263 (1967); D. Cash and T. J. Carew, *J. Neurobiol.* 20, 25 (1989).
 9. J.-y. Wu *et al.*, *J. Neurosci.*, in press.
 10. Y. Tsau *et al.*, *ibid.*, in press.
 11. On the assumption that eight LE neurons responded to a light touch with one or two action potentials (4), the LE contribution to the motor neuron postsynaptic potential was estimated (10) to be about 5% from the relative area under the monosynaptic and polysynaptic postsynaptic potentials. L. E. Trudeau and V. F. Castellucci [*J. Neurosci.* 12, 3838 (1992)] reevaluated the total monosynaptic contribution and arrived at an upper limit of 23%. The LE neuron contribution to this monosynaptic component is uncertain. T. E. Cohen, V. Henzi, E. R. Kandel, and R. D. Hawkins [*Soc. Neurosci. Abstr.* 17, 1302 (1991)] found that LE neurons always fired after the first spike in motor neurons. Finally, the LE neurons are not activated by light touches that do activate the gill withdrawal reflex [S. W. Kaplan, E. R. Kandel, R. D. Hawkins, *Soc. Neurosci. Abstr.* 19, 16 (1993)].
 12. P. Gettings, *Annu. Rev. Neurosci.* 12, 185 (1989).
 13. J. Koester and E. R. Kandel, *Brain Res.* 121, 1 (1977); J. H. Byrne and J. Koester, *ibid.* 143, 87 (1978); J. H. Byrne, *J. Neurophysiol.* 43, 896 (1980); R. D. Hawkins, V. F. Castellucci, E. R. Kandel, *ibid.* 45, 304 (1981); J. H. Byrne, *ibid.* 49, 491 (1983); W. N. Frost, thesis, Columbia University (1987); J. Koester, *J. Neurophysiol.* 62, 1113 (1989); A. Alevizos, K. R. Weiss, J. Koester, *J. Neurosci.* 9, 3058 (1989).
 14. J. J. Hopfield and D. W. Tank, *Science* 233, 625 (1986).
 15. We thank V. Pantani and H. Abildgaard of the Department of Physiology electronics shop for design and construction of the amplifiers and analog-to-digital converter; A. I. Cohen and D. Schiminovich for data analysis software; and A. H.

Cohen, B. Ehrlich, B. Ross, Y. Tsau, and D. Zecevic for comments on the manuscript. Supported in part by grant NS08437 from the National Institute of Neurological Diseases and Stroke, NIH

Research Service Award NS07102, and an IBM fellowship.

1 September 1993; accepted 28 December 1993

In Vivo Ca^{2+} Dynamics in a Cricket Auditory Neuron: An Example of Chemical Computation

Erik C. Sobel and David W. Tank

Fura-2 calcium imaging in the cricket omega neuron revealed increased intracellular free calcium ion concentration in response to simulated cricket calling songs and other sound stimuli. The time course of the increase and decrease in intracellular calcium coincided with the time course of forward masking, a time-dependent modulation of auditory sensitivity. The buffering of calcium transients with high concentrations of a kinetically fast calcium buffer eliminated the post-stimulus hyperpolarization associated with forward masking, whereas the uncaging of calcium inside the neuron produced a hyperpolarization. The results suggest that sound-stimulated intracellular calcium accumulation acts by means of a calcium-activated hyperpolarizing current to produce forward masking. These findings underscore the importance of chemical dynamics in neural computation by demonstrating a behaviorally relevant role of calcium dynamics *in vivo*.

With the advent of techniques for measuring the spatial and temporal dynamics of chemical species in neurons (1), it is possible to ask how the dynamics of chemical activity (such as ion concentration) contribute to neural computation. Here we report how one form of chemical activity, the temporal dynamics of intracellular free calcium ion concentration, $[Ca^{2+}]_i$, in a cricket auditory interneuron, underlies forward masking, a psychophysical and electrophysiological phenomenon in cricket hearing. Forward masking is a form of temporal inhibition in which a loud sound suppresses the response to subsequent sounds (a temporal analog of lateral inhibition). This temporal inhibition may be used for automatic gain control or background subtraction, allowing female crickets to “focus” on the loudest caller in the presence of multiple calling males and background noise. Because this ability would enable the cricket to home in on an individual chirping male, it has been referred to as a form of selective attention (2) in analogy to the “cocktail party phenomenon” observed in human auditory psychophysics (3). An electrophysiological correlate of forward masking is observed in the omega neuron, one of the first interneurons in the cricket auditory pathway. This correlate appears as a long-lasting, post-stimulus hyperpolarization and concomitant reduction in action potentials after sound stimuli (2).

The response of an omega neuron to a simulated calling song and the forward masking effect are shown in Fig. 1 (4). The response to chirps of a single calling song presented at 60-dB sound pressure level (SPL) is shown in Fig. 1A and Fig. 1B shows the

response to two simultaneous calling songs. The chirps of the 90-dB song precede the chirps of the 60-dB song and suppress the number of action potentials elicited by the 60-dB song, compared with the number of action potentials evoked by the 60-dB song by itself. This effect is accompanied by a small hyperpolarization that occurs between chirps. The masking increases from the first to the fourth chirp in the sequence, at which point the action potentials evoked by the quieter calling song are completely eliminated. The hyperpolarization that follows each chirp also accumulates with each successive chirp. Figure 1C summarizes this forward masking effect, showing the number of spikes per chirp in the absence of masking and with two different masking intensities. As the masking intensity is increased the curves shift to the right, showing that the cell's auditory threshold is temporarily raised by the masking stimuli. The amount of masking produced by the 90-dB song on the 60-dB song increases with each subsequent chirp (Fig. 1B), suggesting that the masking effect takes longer to decay than the inter-chirp interval. As a result, the response to later chirps is affected by the residual masking from earlier chirps. This observation and the data in Fig. 1C suggest that the physiological variable that controls masking increases with sound intensity and decays slowly (several seconds), compared to the inter-chirp interval. Forward masking cannot be explained by inhibition from the known connections onto the omega neuron (5). Therefore, we hypothesized that a calcium-activated hyperpolarizing current produces forward masking and, thus, that the dynamics of forward masking are determined by the dynamics of $[Ca^{2+}]_i$.

To investigate this hypothesis, we mea-

Biological Computation Research Department, AT&T Bell Laboratories, Murray Hill, NJ 07974, USA.

sured changes in $[Ca^{2+}]_i$ in response to sound stimuli in the omega neuron in the semi-intact cricket with the fluorescent calcium indicator fura-2 (Fig. 2A). Calcium accumulation was observed during presentations of simulated cricket calling songs at naturally occurring intensities (50- to 100-dB SPL) (Fig. 2B)—the same stimulus conditions that produce the forward masking effect shown in Fig. 1. With the onset of each chirp there was an influx of calcium, most likely through voltage-sensitive calcium channels or ligand-gated channels, which did not completely decay before the next chirp. Consequently, calcium accumulated over the course of the calling song and decayed back to resting level when the calling song ended. Louder chirping produced larger calcium accumulations. This observation suggests that under conditions encountered by a cricket in the wild (multiple chirping males for several hours), $[Ca^{2+}]_i$ in the omega cell approaches a steady state that depends on the recent average sound intensity. A possible role of this elevated calcium in

modulating the auditory neuron's threshold, as in forward masking, is suggested by our finding that the elevated calcium is correlated with a decreased response to sound (Fig. 3A).

To investigate quantitatively the temporal correlation between $[Ca^{2+}]_i$ accumulation and the post-stimulus hyperpolarization that accompanies forward masking, we measured $[Ca^{2+}]_i$ in response to sounds of long duration that elicit larger hyperpolarizations than individual chirps (Fig. 3B). These sounds evoke a large depolarization and brisk firing of action potentials for the entire duration of the sound. Immediately after the sound, the cell shows a deep hyperpolarization that decays back to resting potential with a time course of several seconds (4.3 ± 1.0 s) (6). These sounds also produced a large increase in $[Ca^{2+}]_i$ that returned to resting level with a time course of 4.5 ± 1.4 s (7), thus matching the time

course of the electrophysiologically observed post-stimulus hyperpolarization. In addition to having a similar time constant, both peak calcium concentration and hyperpolarization increased to asymptotic levels as sound intensity and duration were increased.

The tight correspondence among $[Ca^{2+}]_i$, the hyperpolarization produced by sound, and reduced omega cell excitability during stimulation supports the hypothesis that a calcium-activated hyperpolarizing current is the mechanism by which calcium accumulation leads to the forward masking effect. The most likely

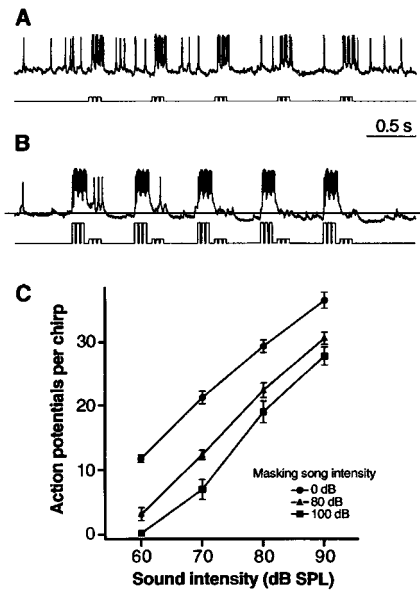


Fig. 1. (A) Intracellular recording from a cricket omega neuron showing the response to chirps of a simulated calling song (60 dB). The upper trace shows the neuron's membrane potential. A chirp is comprised of three syllables (25-ms pulses of 4.8-kHz sound, indicated schematically by square pulses in the lower trace) with an intersyllable interval of 35 ms and an inter-chirp interval of 0.5 s. (B) The response of the same cell to two calling songs (90 dB, large pulses in lower trace, and 60 dB, small pulses in lower trace) illustrating the forward masking effect. (C) Forward masking shifts the omega neuron's input-output function to the right. The number of action potentials per chirp in the quieter song is shown as a function of the quieter song's intensity for three intensities of the masking song. Each data point shows the mean of five chirps. Error bars show standard errors ($n = 8$).

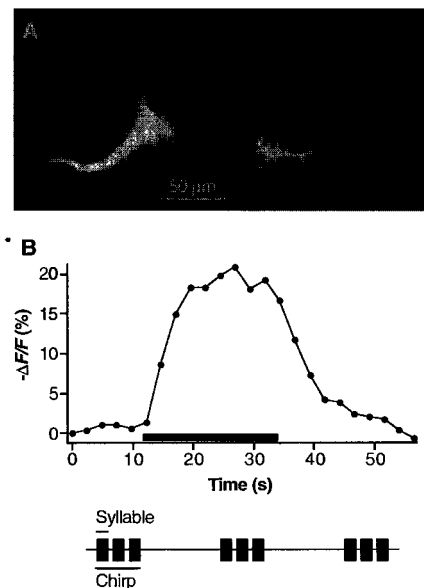


Fig. 2. (A) A CCD (charge-coupled device) fluorescence image of an omega neuron filled with fura-2 (excitation, 385 nm). The cell body is out of focus in the upper left corner. The neurites that receive input from auditory fibers are located in the lower left quadrant. The neurites that form synapses onto the omega neuron's mirror image partner are located in the lower right quadrant. The neuron is located 200 μm beneath the ganglion surface. (B) The accumulation of $[Ca^{2+}]_i$ in an omega neuron in response to a simulated calling song. The solid bar below the graph shows the period during which the calling song was presented. A schematic diagram of the calling song is shown below the axis (4.8-kHz carrier, 25-ms syllable duration, 35-ms syllable period, three syllables per chirp, 0.5-Hz chirp rate). The change in fura-2 fluorescence divided by the absolute fluorescence intensity ($-\Delta F/F$) is monotonically related to intracellular free calcium concentration, and was determined from measurements in a 20 by 20 pixel region of the omega neuron image.

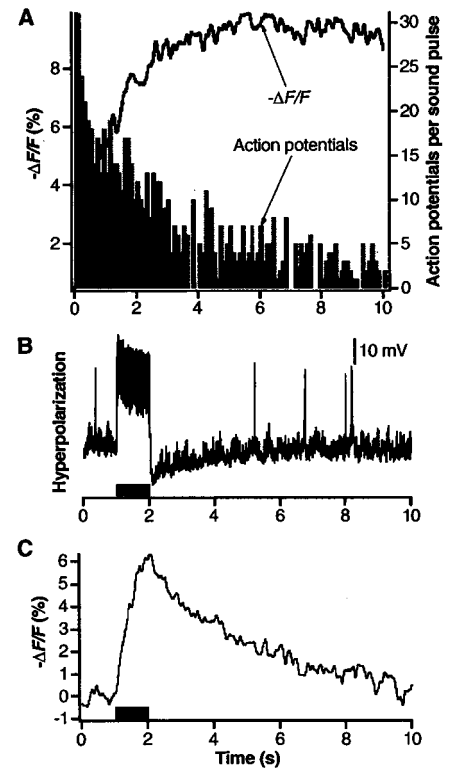


Fig. 3. (A) The accumulation of $[Ca^{2+}]_i$ (bold line) and the corresponding decrease in the number of action potentials per sound pulse (histogram) qualitatively follow the same time course. The cricket was presented with a 4.8-kHz sound amplitude modulated into a pulse train (75-ms pulse duration, 10-Hz repetition rate, 5-ms rise and fall, 90-dB SPL). The train began at the origin. The accumulation of $[Ca^{2+}]_i$ is shown as the percent decrease in fura-2 fluorescence as described in the legend to Fig. 2. The histogram shows the number of action potentials per 75-ms sound pulse. (B) Intracellular recording of a response to a 1-s tone (dark bar; 90-dB SPL, 4.8 kHz) illustrating the post-stimulus hyperpolarization. After the stimulus, the cell shows a hyperpolarization of ~ 10 mV that decays slowly with a time constant of 4.3 s (6). (C) Optical recording of calcium dynamics from the same cell as in (B). The graph shows the absolute fluorescence intensity, which is monotonically related to $[Ca^{2+}]_i$, measured with a photodiode during the same conditions as in (B) (stimulus presentation indicated by the solid bar above the abscissa) (15).

candidate for such a current is a calcium-activated potassium current such as those demonstrated in *Drosophila* (8), in the large monopolar cells of the fly optic lobe (9) as well as in cockroach motor neurons (10).

To test the involvement of a calcium-dependent potassium conductance in the post-stimulus hyperpolarization, we injected the omega cell with a high concentration of fura-2. Moderate concentrations of kinetically fast, high-affinity calcium buffers like fura-2 are known to block calcium-activated potassium channels in other preparations (11). Omega neurons filled with a high concentration of fura-2, unlike normal omega cells, continued to fire for several seconds after the termination of the sound stimulus and showed a reduced post-stimulus hyperpolarization (Fig. 4, A and B). This behavior suggests that a calcium-activated current is necessary for the production of the hyperpolarization observed in normal cells. Additional evidence of

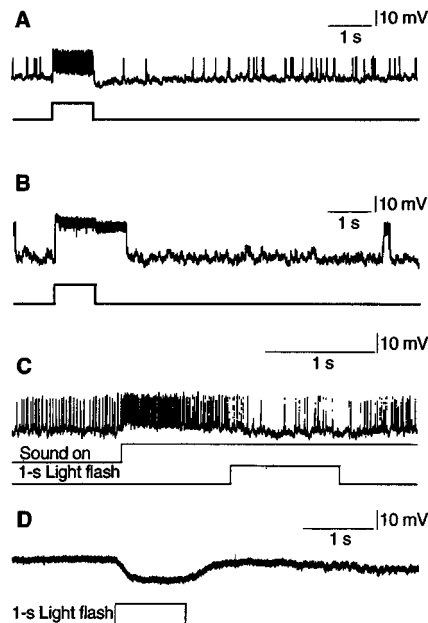


Fig. 4. Electrophysiological response of an omega cell to a 1-s tone (95-dB SPL, 4.8 kHz) (A) before and (B) after the filling of an omega neuron with a high concentration of fura-2 (16). (C and D) Electrophysiological response of an omega neuron to calcium released intracellularly by photolysis of DM-Nitrophen. (C) Upper trace, membrane potential. The middle trace shows the onset of a continuous 4.8-kHz tone. The lower trace shows the open time of a shutter that allowed ultraviolet light to illuminate the omega neuron and release the calcium bound to DM-Nitrophen. The firing rate of the cell in response to the sound is reduced by increased intracellular calcium. (D) Upper trace, membrane potential. The lower trace shows the open time of the shutter as in (C). In the absence of sound-induced depolarization, a larger hyperpolarization is observed in response to the release of caged calcium. (C) and (D) show data from different cells.

a calcium-activated current was obtained with DM-Nitrophen, a caged calcium compound, which releases calcium upon photolysis (12) and transiently raises $[Ca^{2+}]_i$. When calcium was released inside omega neurons through this method, a transient hyperpolarization and decreased sensitivity to sound were observed (13) (Fig. 4, C and D).

The omega cell responds to sound stimuli including species-specific sounds with an accumulation of $[Ca^{2+}]_i$ that depends on the intensity and duration of sound and that decays slowly (3- to 5-s time constant). The accumulation of $[Ca^{2+}]_i$ reflects the average environmental sound level through its "leaky integrator" dynamics. Our data suggest that the integration and decay times of $[Ca^{2+}]_i$ accumulation give rise to the temporal dynamics of forward masking by activating a hyperpolarizing current, temporarily raising the neuron's threshold and shifting its input-output function (action potentials per decibel of sound). The dynamics of $[Ca^{2+}]_i$ accumulation and decay have a neuroethological significance because hyperpolarization of individual omega neurons in crickets (*Gryllus bimaculatus*) that are actively engaged in tracking calling songs reduces the crickets' tendency to turn toward calling songs on the hyperpolarized side (14). Our findings provide a simple example of chemical computation in central nervous system function by illustrating how the dynamics of a chemical species can be used to perform a useful transformation of information.

REFERENCES AND NOTES

1. R. Y. Tsien, *Annu. Rev. Neurosci.* **12**, 227 (1989); D. W. Tank, M. Sugimori, J. A. Connor, R. R. Llinás, *Science* **242**, 773 (1988); A. Borst and M. Egelhaaf, *Proc. Natl. Acad. Sci. U.S.A.* **89**, 4139 (1992).
2. G. S. Pollack, *J. Neurosci.* **8**, 2635 (1988).
3. E. C. Cherry, *J. Acoust. Soc. Am.* **25**, 975 (1953).
4. Crickets (*Acheta domestica*) were waxed ventral side up with their forelegs inserted into leg phones [H.-U. Kleindienst, U. T. Koch, D. W. Wohlers, *J. Comp. Physiol. A* **141**, 283 (1981)]. The cuticle over the prothoracic ganglion was removed. The ganglion was desheathed and supported as described in (14). Intracellular recording and dye filling were made with glass capillary microelectrodes [1.0 mm by 0.58 mm borosilicate glass, filled at the tip with 28 mM fura-2 pentapotassium salt (Molecular Probes) in 150 mM potassium acetate and backfilled with 150 mM potassium acetate]. The preparation was perfused with oxygenated saline containing a bicarbonate buffer. Sound stimuli were generated by a synthesized function generator gated by a pulse generator and passed through a cosine switch and precision attenuators. Simulated calling songs consisted of a 4.8-kHz sine wave amplitude-modulated into chirps composed of three pulses (syllables), each with a 25-ms duration and a 35-ms period with rise and fall times of 5 ms. Sound intensities were calibrated (in decibels SPL rms) with a Bruel & Kjaer 4136 microphone and HP35665A dynamic signal analyzer.
5. A. I. Selverston, H.-U. Kleindienst, F. J. Huber, *J. Neurosci.* **5**, 1283 (1985).
6. The characteristic decay times determined from single exponential fits (22 measurements from seven crickets) were averaged to produce the reported time constant. The optical recording methods used in these experiments are similar to those reported by W. G. Regehr and D. W. Tank [*ibid.* **12**, 4202 (1992)]. The omega neuron was filled with the calcium indicator fura-2 by the passing of a 0.75- to 1.0-nA hyperpolarizing current for ~10 min. The electrode was removed and the fura-2 was allowed to diffuse for at least 20 min. The cell was imaged through an upright epifluorescence microscope (Zeiss, Axioskop; 100-W Hg lamp, 385-nm excitation, 405-nm dichroic, 495-nm long-pass barrier filter). Fluorescence was imaged with a microcomputer-controlled cooled CCD camera (CH220, Photometrics). For Fig. 2, a photodiode (Hamamatsu, S1087-01) was used in place of the camera for increased temporal resolution. The field of view of the photodiode was 65 μ m by 65 μ m centered on the branch of the neurite in the lower left quadrant of Fig. 2A. The photodiode output was amplified, low pass-filtered (25-ms time constant), and sampled (5-kHz sample rate) by a microcomputer. An additional digital Gaussian filter ($\sigma = 70$ ms) was applied to the data. In CCD data, background fluorescence from an area adjacent to the cell was subtracted before the percent change was computed. In photodiode experiments, background subtraction was not performed. Increased calcium leads to a decrease in fluorescence with 385-nm excitation. Both CCD and photodiode data were corrected for bleaching (~1% per 15 s) by linear extrapolation. The change in 385-nm fluorescence measured by the photodiode was reduced by high autofluorescence in the tissue, lack of background subtraction, and spatial averaging over regions of neuropil other than the filled dendrites of the omega cell. Changes observed with the CCD camera were larger because background subtraction was performed and the fluorescence measurements could be restricted to the fura-2-filled neurites of the omega cell.
7. The characteristic decay times determined from single exponential fits (53 measurements from seven crickets) were averaged to produce the reported time constant.
8. B. Ganetzky and C.-F. Wu, *Trends Neurosci.* **8**, 322 (1985).
9. R. C. Hardie and M. Weckstrom, *J. Comp. Physiol. A* **167**, 723 (1990).
10. M. V. Thomas, *J. Physiol.* **350**, 159 (1984); D. Yamamoto, R. D. Pinnock, D. B. Sattelle, *J. Neuroendocrinol.* **1**, 89 (1989).
11. For example, see W. M. Roberts, *Nature* **363**, 74 (1993).
12. L. Lando and R. S. Zucker, *J. Gen. Physiol.* **93**, 1017 (1989); S. R. Adams and R. Y. Tsien, *Annu. Rev. Physiol.* **55**, 755 (1993); G. C. R. Ellis-Davies and J. H. Kaplan, *J. Org. Chem.* **53**, 1966 (1988).
13. Omega neurons were impaled with electrodes filled at the tip with 100 mM DM-Nitrophen (Calbiochem) and 10 mM Sulforhodamine 101 (Sigma) (for identification of filled neurons). The neurons were filled by the passing of -0.5 to -1.0 nA of current for 5 to 10 min. To photolyze the DM-Nitrophen, the ganglion was exposed to light from a 100-W mercury arc lamp band-pass-filtered between 340 to 400 nm. Light exposures were 1 s long. Hyperpolarization or decreased response to sound was not observed in response to light flashes in the absence of DM-Nitrophen and was not observed after two or three flashes, at which point all of the caged calcium was probably released. After the hyperpolarization accompanying the uncaging of calcium, a slow depolarization was observed that lasted for several seconds. This depolarization did not appear to be due to Ca^{2+} because it could be elicited repeatedly after all the Ca^{2+} was presumably uncaged and was most likely an artifact of the light flash, the photolysis products of the DM-Nitrophen, or both [A. M. Gurney, in *Fluorescent and Luminescent Probes for Biological Activity: A Practical Guide to Technology for Quantitative Real Time Analysis*, W. T. Mason, Ed. (Academic Press, London, 1993), pp. 335-348].
14. K. Schildberger and M. Horner, *J. Comp. Physiol. A* **163**, 621 (1988).
15. In most experiments, imaging was performed

with a CCD camera ($n = 6$). The photodiode data are shown because they provide greater time resolution.
 16. The electrode tip was filled with 28 mM fura-2 in

150 mM potassium acetate that was iontophoresed for 55 min with a -1 -nA current.
 17. We thank R. Hoy, G. Pollack, and K. Schildberger for helpful discussions and advice and A. Gel-

perin, K. Delaney, R. Yuste, and M. Feller for their helpful comments on the manuscript.

23 September 1993; accepted 16 December 1993

Prevention of Vertebrate Neuronal Death by the *crmA* Gene

Valeria Gagliardini, Pierre-Alain Fernandez, Robert K. K. Lee, Hannes C. A. Drexler, Rocco J. Rotello, Mark C. Fishman, Junying Yuan*

Interleukin-1 β converting enzyme (ICE) is a mammalian homolog of CED-3, a protein required for programmed cell death in the nematode *Caenorhabditis elegans*. The activity of ICE can be specifically inhibited by the product of *crmA*, a cytokine response modifier gene encoded by cowpox virus. Microinjection of the *crmA* gene into chicken dorsal root ganglion neurons was found to prevent cell death induced by deprivation of nerve growth factor. Thus, ICE is likely to participate in neuronal death in vertebrates.

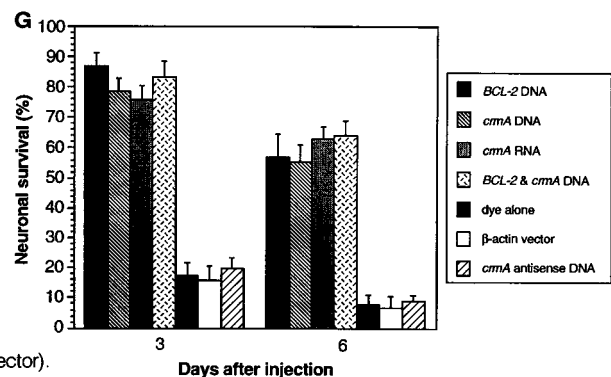
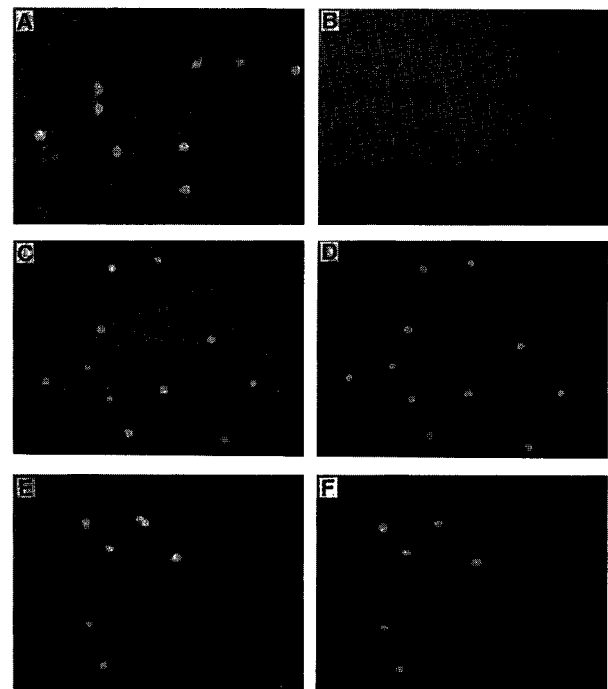
(injected with dye alone, vector alone, or antisense *crmA* cDNA) died, with fewer than 10% surviving to day 6 (Fig. 1). In contrast, more than 60% of the *crmA*-injected neurons survived through day 6 in the absence of NGF (Fig. 1).

Expression of *crmA* protein was detected in almost all of the injected neurons by immunofluorescence staining with an affinity-purified rabbit polyclonal antibody to *crmA* (Fig. 2) (8). The *crmA* protein could be detected in neurons 9 days after injection, suggesting that it is very stable. The *crmA*-injected DRG neurons cultured in the absence of NGF were round and often devoid of extensive neurites, a morphology similar

The survival of sensory neurons during development of the vertebrate nervous system depends on neurotrophic factors produced by the neuronal targets (1). In the absence of these factors, the neurons are thought to undergo programmed cell death, an active process requiring RNA and protein synthesis (2). Little is known about the genes regulating cell death in vertebrates. A gene essential for cell death in the nematode *C. elegans*, *ced-3*, was recently shown to share sequence similarity with a mammalian gene, *ICE*, which encodes a cysteine protease involved in the processing of interleukin-1 β (3). Overexpression of *ICE* induces programmed cell death in Rat1 fibroblasts and this death can be suppressed by the cowpox virus *crmA* gene, a specific inhibitor of *ICE*, and by the *BCL-2* proto-oncogene (4, 5). To determine whether *ICE* is involved in neuronal death, we investigated the effect of *crmA* on the survival of chicken dorsal root ganglion (DRG) neurons cultured in the absence of nerve growth factor (NGF), a condition that would normally lead to cell death.

We microinjected an expression vector (pHD1.2) containing a *crmA* complementary DNA (cDNA) under the control of the chicken β -actin gene promoter, or in vitro transcribed *crmA* RNA (6), into cultured DRG neurons along with rhodamine-isothiocyanate-labeled dextran (7). About 90% of the injected neurons retained a normal morphology, and, in the presence of NGF, about 85% survived through day 6. Within 3 days of NGF deprivation, however, more than 80% of the control neurons

Fig. 1. Effects of *crmA* and *BCL-2* on the survival of NGF-deprived DRG neurons in culture. The neurons were microinjected with a control β -actin vector (A and B), an expression vector containing *crmA* cDNA (C and D), or an expression vector containing *BCL-2* cDNA (E and F). The neurons were photographed after being cultured in the absence of NGF for 0 days (A, C, and E) or 3 days (B, D, and F). Photographs were taken with a computerized video imaging system (Axovideo, Axon Instruments) with a rhodamine filter. Images of the fluorescent cells were amplified with a Silicon-Intensified-Target (SIT) video camera (Dage). (G) shows the survival of DRG neurons in the absence of NGF after injection of *BCL-2* expression vector RR/1 (*BCL2* DNA), *crmA* expression vector pHD1.2 (*crmA* DNA), antisense-*crmA* expression vector pHD2.1 (*crmA* antisense DNA), *crmA* RNA, *BCL-2* expression vectors RR/1 and *crmA* pHD1.2 (*BCL-2* and *crmA* DNA), control β -actin vector (p β actiSTneoB), or dye alone. Live DRG neurons were scored as rhodamine-containing cells with neuronal morphology. Trypan blue staining was used to confirm the viability of neurons in some of the experiments (data not shown). Results are presented as the mean percentage of survival \pm SEM, observed in four to five experiments (\sim 300 microinjected neurons for each vector).



Cardiovascular Research Center, Massachusetts General Hospital, 149 13th Street, Charlestown, MA 02129, USA, and Department of Medicine, Harvard Medical School, Boston, MA 02115, USA.

*To whom correspondence should be addressed.